Validation of 525 nm and 1020 nm aerosol extinction profiles derived from ACE imager data: comparisons with GOMOS, SAGE II, SAGE III, POAM III, and OSIRIS

F. Vanhellemont, C. Tetard, A. Bourassa, M. Fromm, J. Dodion, D. Fussen, C. Brogniez, K. L. Gilbert, D. N. Turnbull, P. Bernath, et al.

Atmos. Chem. Phys. Discuss., 7, 12349–12379, 2007
www.atmos-chem-phys-discuss.net/7/12349/2007/

Atmospheric Chemistry and Physics Discussions

Validation of 525 nm and 1020 nm aerosol extinction profiles derived from ACE imager data: comparisons with GOMOS, SAGE II, SAGE III, POAM III, and OSIRIS

F. Vanhellemont[1], C. Tetard[2], A. Bourassa[3], M. Fromm[4], J. Dodion[1], D. Fussen[1], C. Brogniez[2], K. L. Gilbert[5], D. N. Turnbull[5], P. Bernath[5,6], C. Boone[5], and K. A. Walker[5,7]

[1]Belgian Institute for Space Aeronomy, Ringlaan 3, 1180, Brussels, Belgium
[2]LOA, Université de Science et Technologies de Lille, Bâtiment P5, 59655 Villeneuve d'Ascq Cedex, France
[3]University of Saskatchewan, 116 Science Place, Saskatoon, SK S7N 5E2, Canada
[4]Naval Research Lab, 4555 Overlook Ave. SW, Washington, DC 20375 USA
[5]Department of Chemistry, University of Waterloo, 200 University Avenue West, Waterloo, Ontario, N2L 3G1, Canada
[6]Department of Chemistry, University of York, Heslington, York, YO10 5DD, UK
[7]Department of Physics, University of Toronto, 60 St. George Street, Toronto, Ontario M5S 1A7, Canada

Received: 12 July 2007 – Accepted: 27 July 2007 – Published: 21 August 2007

Correspondence to: F. Vanhellemont (filip.vanhellemont@aeronomie.be)

Abstract

The Canadian ACE (Atmospheric Chemistry Experiment) mission is dedicated to the retrieval of a large number of atmospheric trace gas species using the solar occultation technique in the infrared and UV/visible spectral domain. However, two additional solar disk imagers (at 525 nm and 1020 nm) were added for a number of reasons, including the retrieval of aerosol and cloud products. In this paper, we present the first validation results for these imager aerosol/cloud optical extinction coefficient profiles, by intercomparison with profiles derived from measurements performed by 3 solar occultation instruments (SAGE II, SAGE III, POAM III), one stellar occultation instrument (GOMOS) and one limb sounder (OSIRIS). The results indicate that the ACE imager profiles are of good quality in the upper troposphere/lower stratosphere, although the aerosol extinction for the visible channel at 525 nm contains a significant negative bias at higher altitudes, while the profiles are systematically too high at 1020 nm. Both problems are probably related to ACE imager instrumental issues.

1 Introduction

The Canadian ACE instruments (Atmospheric Chemistry Experiment; see Bernath et al., 2005) on SCISAT-I are primarily intended to derive concentration profiles for a large number of trace gases, with the aim of studying chemical and physical processes that control ozone in the upper troposphere and lower stratosphere at mid- and high latitudes. Temperature, pressure and neutral density profiles are also target quantities, as well as aerosol and cloud extinction profiles. ACE is equipped with a high spectral resolution (0.02 cm^{-1}) Fourier Transform Spectrometer (FTS) using the solar occultation technique, in the 2.2 to 13.3 μm spectral range. UV/Vis solar occultation measurements are provided by the MAESTRO instrument (Measurement of Aerosol Extinction in the Stratosphere and Troposphere by Occultation; see McElroy and et al., 2007), a dual diffraction grating spectrometer operating in the 285–1020 nm spectral

ACPD

7, 12349–12379, 2007

range, with a resolution of 1–2 nm, depending on wavelength.

Additionally, two imaging channels are included (Gilbert et al., 2007). These consist of a pair of filtered CMOS detector arrays that are able to record images of the Sun at 525 and 1020 nm. There are several reasons for the existence of these two imagers. (1) They provide an important diagnostic for the variation of the flux over the distorted solar disk. (2) They provide an important diagnostic for pointing, and are key to the characterization of the onboard suntracker. (3) Aerosol and cloud data products can be derived from the solar extinction. This last reason motivates the choice of wavelengths: at 525 and 1020 nm, the measurements match two of the 7 channels of the SAGE II satellite instrument (Russell and McCormick, 1989).

The ACE mission was launched on 12 August 2003. Science commissioning was carried out in January 2004, and routine operation started in February 2004. Since then, ACE has continuously provided measurements. At the time of writing, only MAESTRO, the ACE imagers and GOMOS provide occultation measurements of stratospheric aerosols and clouds in the UV/Visible, while the majority of other occultation instruments (POAM III, SAGE II, SAGE III, HALOE) have been switched off or have failed. In order to provide continuity in the long term data record of stratospheric aerosols and high-altitude clouds, the remaining instruments are very important. The ACE imager data offer an additional advantage, since it is in principle possible to observe aerosols and clouds on a two dimensional field. This feature allows the identification of particle/cloud types by the use of the observed morphology (cloud shape, layer dimensions). Initial studies on this topic have already been performed by Dodion et al. (2007).

The subject of this paper is the validation of the aerosol and cloud extinction profiles that are derived from the two ACE imager measurements, by comparison with results from four satellite occultation instruments (SAGE II, SAGE III, POAM III and GOMOS) and one limb sounder (OSIRIS). We will first give a basic description of the ACE imagers, and point out some currently known problems in the observations and data processing. Then, a brief description for the other instruments is given, and the

comparisons with the ACE imager profiles are presented. Finally, in the conclusions, we attribute the differences in the comparisons to a number of possible instrumental and observational causes.

2 The ACE imagers

A detailed description of the ACE imagers and the retrieval process can be found in Gilbert et al. (2007). However, for the purpose of this paper, it is necessary to repeat the essentials here. The two imagers are identical, except for the filters (see Fig. 1): the VIS filter is centered at 527.11 nm (13.28 nm FWHM) and the NIR filter at 1020.55 nm (19.44 FWHM). Incoming solar light is first passed through a neutral density filter to prevent detector saturation when looking at the unattenuated high sun. The light is then split in two parts, and sent to each imager. Both detectors have an imaging area of 256x256 pixels. After readout, the pixels are binned to produce an effective 128x128 pixel array, of which only 64×64 pixels containing the Sun's image are retained. During occultation, such a 64×64 pixel image is recorded every 0.25 seconds.

The total field-of-view (FOV) of both imagers is 30 mrad, to be compared to the 9 mrad angular diameter of the Sun. The signal-to-noise ratio (SNR) is very good (about 1500 for an image pixel at the centre of the unattenuated high Sun). Also, detector dark current is well characterized by measurements from columns of pixels covered with a metallic layer to prevent light penetration.

Still, some significant problems remain to be addressed. (1) During an occultation, there is an anomalous linear increase in the response of the detectors. The effect is much more pronounced for the NIR than for the VIS imager. It is not caused by solar heating, and therefore involves the operation of the detector itself. A correction is applied for the entire occultation, based on an extrapolation of the signal increase outside the atmosphere. However, it is uncertain how accurate this correction is. (2) A more serious problem involves the optics rather than the detectors. Both imagers suffer from overlapping multiple images, caused by reflections from the neutral density

ACPD
7, 12349–12379, 2007

EGU

filter. Most problematic are the reflected images overlapping the main Sun image (that is used to calculate atmospheric transmission). Furthermore, the position and shape of the secondary images change during the occultation. It is as yet undetermined how much signal the sum of the reflected images contributes to the main image; around the edge of the main solar disk image, the contribution is about 5–8%. (3) The NIR imager is out of focus and produces a distorted image, for unclear reasons.

The calculation of total extinction profiles is carried out as follows. First, all images are corrected for dark current and the anomalous intensity increase of the detectors. Then, 144 high Sun images are averaged to produce one high SNR reference image, that is used as the divisor in the transmittance calculation. All images are subsequently rotated about their respective sun centroids so that the Earth's horizon is parallel to the imager horizontal axis. Because of refractive solar disk flattening, one pixel in a low Sun image corresponds to multiple pixels in the same column of the high Sun image. This pixel mapping has proven to be far from straightforward and currently an approximation is used which sidesteps the problem. Only 3 pixels centred on the co-registred ACE-FTS FOV are being analysed. They all are located in the geometric centre of the high Sun image, where the solar limb darkening curve is relatively flat, and are associated with the same tangent height, interpolated from those that are assigned to the FTS measurements. Relative accuracy of the tangent heights is about 150 m. After calculation of the transmittance, total extinction profiles (on an altitude grid with 1 km spacing) are obtained with a spatial inversion procedure that is identical to the one used for the FTS.

At present, the processing code for the ACE imager data is in a preliminary state, as was mentioned by Gilbert et al. (2007). It is important to take this in account during inspection of the results shown in this work.

3 Aerosol extinction profiles from the ACE imagers

At present, no official ACE aerosol extinction data product has been delivered yet. Instead, total extinction profiles are available, directly calculated from the imager transmittances as described above. However, aerosol extinction is easily obtained. Considering the fact that the ACE FTS and the imagers are optically aligned and are viewing the same central part of the solar disk, the gas extinction contributions (O_3, NO_2, neutral density) can be obtained from the FTS gas retrieval data set. Ozone and NO_2 volume mixing ratios were taken from the version 2.2 ACE-FTS data set (including updates for ozone, HDO and N_2O_5) and converted to number density profiles. Ozone and NO_2 cross sections, as measured by the SCIAMACHY instrument (Bogumil et al., 1999) were chosen, while the paper by Bodhaine et al. (1999) provided accurate up-to-date Rayleigh cross sections. Since the filter functions for both imager channels are relatively broad (see Fig. 1), a convolution was necessary: all cross sections and filter functions were interpolated on a fine spectral grid (0.01 nm resolution), multiplied and integrated. Gas optical extinction profiles were subsequently calculated, and subtracted from the imager total extinction measurements, resulting in aerosol extinction profiles.

It should be mentioned here that the aerosol extinction coefficients obtained at 525 and 1020 nm are actually filter-convolved extinction coefficients. However, since typical aerosol extinction spectra change smoothly with wavelength, the differences between the convolved and true aerosol extinction coefficients will be minimal.

4 ACE imager validation

In all individual instrument comparisons in this paper, we will show the statistics (mean and standard deviation, or alternatively, median, 16th and 84th percentiles) for the coincidence data set, and the percent relative difference between the two instruments, calculated with respect to the average of both instruments. For instance, the relative

difference for the i-th ACE imager and GOMOS coincidence is calculated as:

$$d_i = 100\% \times 2 \left(\frac{p_i^{\mathrm{ACE}} - p_i^{\mathrm{GOMOS}}}{p_i^{\mathrm{ACE}} + p_i^{\mathrm{GOMOS}}} \right) \quad (1)$$

The advantage of this expression lies in the fact that the relative difference does not diverge when one of the profiles becomes small with respect to the other one, which is indeed the case as will be shown later. On the other hand, one should be careful with the interpretation: if p_i^{GOMOS} goes to zero while p_i^{ACE} is negative (bias), the relative difference will be a large positive value, which can lead to the wrong conclusion that p_i^{ACE} is larger than p_i^{GOMOS}.

We will show comparisons from very low tropospheric to very high stratospheric altitudes (from 5 to 40 km). The high altitudes are presented because some instrumental/retrieval issues become very clear in this region. The lower altitude results below the tropopause should be taken with caution: the troposphere is a very dynamical, complicated area, filled with inhomogeneities and even coincidences may not be very informative. Therefore, stratospheric comparisons are our main focus of interest.

4.1 GOMOS comparisons

GOMOS (Global Ozone Monitoring by Occultation of Stars Bertaux et al., 1991; Kyrölä et al., 2004) is a stellar occultation instrument operating in the UV, Vis and NIR wavelength range. Equipped with a telescope and star tracker, it continuously measures light from a wide variety of stars that are setting behind the Earth horizon. Two grating spectrometers record the spectra, within a total wavelength range from 248 nm to 954 nm. For the purpose of this paper only the first spectrometer A (248 nm to 690 nm) is important; it is mainly intended to retrieve concentration profiles for ozone, NO_2, NO_3, Na, OClO and particle extinction profiles (stratospheric aerosols, cirrus, polar stratospheric clouds). The upper wavelength limit of 690 nm implies of course that it is impossible to compare GOMOS and ACE aerosol extinction values at 1020 nm.

GOMOS is one of the three instruments used for atmospheric research onboard the European ENVISAT satellite. A good latitudinal and longitudinal coverage is obtained, with a global coverage of roughly 3 days. Since the launch date (1 March 2002), GOMOS typically has measured about 100 000 occultations per year. This considerable number is due to the large number of stars available, and compensates for the relatively low SNR that is caused by the low intensity of star light.

In a first spectral inversion step, the retrieval algorithm inverts transmittances to slant path integrated densities for the gases and optical thickness for the aerosols. In this step, the aerosol extinction spectra are modeled as quadratic polynomials of wavelength. The second step consists of the spatial inversion to gas concentration and aerosol extinction profiles. A number of parameters determine the final GOMOS retrieval accuracy. The star magnitude determines the overall brightness of the star light. Star temperature on the other hand controls the spectral range where the maximum emission of light occurs. Less intuitive but equally important is the occultation obliquity with respect to the Earth horizon: vertical occultations can be perfectly corrected for star scintillation, while retrievals from oblique occultations suffer from residual, imperfectly corrected scintillation (Fussen et al., 2005). However, these residual perturbations tend to cancel out when taking averages.

In this validation study, we have excluded the use of aerosol extinction profiles, derived from day-side (bright limb) occultations; at present, the quality of these profiles is far from excellent because the bright limb spectral signature severely perturbs the extinction retrievals. Therefore, only nighttime occultations were used. Furthermore, it is impossible to probe the aerosols in the lower stratosphere using weak stars since the measured signal drops below the instrument sensitivity at a rather high altitude (cut-off). We therefore decided to use only occultations of stars with a magnitude smaller than 2.

While ACE always measures at the Sun terminator, the GOMOS occultations occur at all local times. Together with the removal of bright limb and weak star measurements, this fact forced us to take a rather large spatio-temporal window (12 h time difference,

500 km) to obtain a total of 225 ACE/GOMOS coincidences within the period from February 2004 to December 2005. Although the temporal difference is large, the spatial distance criterion of 500 km is reasonable since the effective slant path through the atmosphere is about this size.

Individual GOMOS aerosol retrievals exhibit a large range of retrieval accuracies, caused by the differences in star magnitude and temperature. For example, at an altitude of 20 km, the 525 nm retrieval accuracies of the coincidence data set range from 1% to 100%. Using the statistical mean and standard deviation as estimators is therefore not a good idea, since they are strongly influenced by the occasional outlier. A better way to estimate the central tendency of a data set is provided by the median, and the spread of the distribution is well represented by the 16th and 84th percentile.

Figure 2 shows the statistics for the 525 nm GOMOS/ACE coincidence ensemble, separately for the Northern (NH) and Southern (SH) hemisphere (126 and 99 profiles, respectively). Immediately clear are the systematically lower values for ACE at higher altitudes. Above 23 to 25 km, these values are even negative. In the upper troposphere and lower stratosphere, the median profiles and statistical spreading for both instruments are very similar at 525 nm. For the NIR channel, GOMOS median values are systematically larger. The median, 16th and 84th percentile for the relative differences are presented in Fig. 3, clearly showing a small negative bias of 20 to 30% from 12 to 24 km (NH) and 12 to 22 km (SH).

4.2 SAGE II comparisons

The solar occultation instrument SAGE II (Stratospheric Aerosol and Gas Experiment II; see e.g. Chu et al., 1989) was launched in October 1984 on the Earth Radiation Budget Satellite (ERBS) to measure 1 km resolution altitude gas concentration profiles and aerosol extinction profiles, using seven spectral passbands centered at 385, 448, 453, 525, 600, 940 and 1020 nm. The instrument had approximately 30 measurement opportunities (sunrise and sunset) each day. Near-global coverage (80° S–80° N) was achieved over time spans of about 1 month. The instrument mission was terminated

on 8 September 2005. Since the spectral domains of the ACE imagers were chosen to agree with two of the SAGE II channels, the aerosol extinction profiles of the two data sets are directly comparable. Details about the SAGE II inversion algorithm can be found in (Chu et al., 1989; Thomason et al., 2007). Basically, the effect of Rayleigh scattering is removed by calculating its contribution from NCEP temperature and pressure data. Following this, the remaining optical depth is separated into contributions from the different species using a least-squares approach.

For the ACE/SAGE II comparison, the coincidence window was chosen to be 400 km in distance, and 2 hours in time. These criteria provided 42 coincidences in the NH and 86 in the SH, for the overlapping period of instrument operation. Profile statistics for each instrument are shown in Fig. 4. Again, at 525 nm we observe systematically negative ACE aerosol extinction values above about 25 km. Below this altitude, the two data sets span similar value ranges, although the mean values differ considerably in the SH. At 1020 nm, profile statistics are very similar in the stratosphere, but SAGE II shows significantly larger mean values below about 18 km. The situation becomes more clear when we observe the relative differences in Fig. 5. At 525 nm, good agreement is found between both instruments below 20–22 km, although there is a positive bias in the NH and a negative bias in the SH. At 1020 nm, both instruments agree even better, but ACE values are systematically larger than the ones from SAGE II, all the way up to 25 or 30 km.

4.3 SAGE III comparisons

The Stratospheric Aerosol and Gas Experiment (SAGE) III (see e.g. Yue and Wang, 2005) is a spectroradiometer developed by NASA, and was launched in December 2001 onboard the Russian Meteor-3M satellite in a Sun synchronous orbit (inclination is about 99.53°) allowing latitude coverage from 45° to 80° in the NH and 35° to 60° in the SH. SAGE III is equipped with a linear CCD array covering the 280–1020 nm wavelength range and with a single photodiode centered at 1545 nm. Using the solar occultation technique, SAGE III measurements allow the retrieval of vertical profiles of

ozone, nitrogen dioxide and aerosol extinctions at nine wavelengths (385, 450, 525, 600, 675, 750, 875, 1020 and 1545 nm). The SAGE III mission was terminated in December 2005.

The inversion algorithm (Rind et al., 2002; Yue and Wang, 2005) starts by performing a molecular scattering correction of the slant path optical thickness. Then multiple linear regressions are performed to obtain slant path density profiles for ozone and nitrogen dioxide in the 440 and 600 nm spectral regions. Aerosol slant path optical thicknesses are then retrieved at each channel by removing the contributions of ozone and nitrogen dioxide. Finally, a modified Chahine method is employed to obtain local gas concentration and aerosol extinction profiles. For this work we are using the SAGE III version 4.0 aerosol products. Two channels (525 nm and 1020 nm) are available for direct comparison with the ACE imager aerosol extinction coefficients.

For the comparison of ACE and SAGE III aerosol extinction profiles, coincidences were searched for between the start of the ACE mission (February 2004) and the end of the SAGE III mission (December 2005). The NH and SH were considered separately, while no seasonal effects were studied. The coincidence criteria were taken to be 400 km spatially and 2 h temporally, resulting in 548 coincidences in the NH and 81 in the SH. The altitude range for comparison was limited to the 5–40 km range; at lower altitudes, both instruments experience a signal cut-off, while at higher altitudes, the aerosol levels are too low to be detected. Possible Polar Stratospheric Cloud (PSC) detections were discarded (temperatures lower than 198 K, high latitude winter), since the different line-of-sights for both instruments are likely to result in a larger statistical spread of the comparisons.

The resulting statistical distributions are shown in Fig. 6. Once again, we observe systematically negative values for ACE at 525 nm above 25 km, and reasonable agreement between the two instruments within the altitude range from 15 to 25 km. Notice the strong variability of ACE at 525 nm in the NH, caused by a significant amount of suspicious values in the coincidence data set. At 1020 nm, we observe a striking resemblance between the profile shapes for ACE and SAGE III, although ACE exhibits

slightly larger values in the altitude range above 13 km. The mean and standard deviation of the set of relative differences are presented in Fig. 7, clearly showing acceptable agreement at 525 nm within the altitude range from 13 to 21 km, and a positive bias at 1020 nm at all altitudes, with the exception of a negative peak at 20 km in the SH.

4.4 POAM III comparisons

POAM III (Polar Ozone and Aerosol Measurement), a solar occultation instrument onboard the SPOT 4 satellite, was launched on 23 March 1998 (Lucke et al., 1999) to observe sunsets and sunrises from a Sun synchronous orbit, ensuring that most occultations occur within 40 degrees from the poles. The instrument has nine separate optical channels, each one equipped with a narrowband interference filter (with center wavelengths at 354, 439.6, 442.2, 603, 761.3, 779, 922.4, 935.9, and 1018 nm), and a silicon photodiode. The FOV is determined by a field stop in the form of a long narrow slit extending horizontally across the entire solar disk, but limiting the vertical view to about 0.77 km at the tangent point. The line-of-sight instrument pointing is controlled by a suntracker that always ensures very accurate knowledge of the slit position on the solar disk. Measurements of the direct sun show SNRs of better than 10 000. POAM III operations ended in December 2005.

The retrieval process starts with transmittance calculations using sun observations outside the atmosphere as reference. Then, the slant path integrated column density of trace gases and aerosol optical thickness are retrieved with a nonlinear optimal estimation method. In this spectral inversion step, aerosol optical thickness is modelled as a quadratic polynomial of the logarithm of wavelength. Local gas concentration and aerosol extinction profiles are finally obtained with a standard spatial inversion code. Typically, the vertical resolution of the aerosol extinction profile at 1020 nm is better than 2 km from 15 to 24 km, and the measurement precision is better than 20% up to 28 km.

For the ACE/POAM III comparisons, coincidence criteria were taken from a previous POAM III validation study (Randall et al., 2001): a window of 4 degrees in latitude

(about 445 km), 12 degrees longitude and 2 h was used. A total of 277 coincidences were found spanning a period from March 2004 to November 2005. Because POAM III measures ocultations in the polar regions, comparisons are particularly difficult since the large aerosol gradients at the edge of the vortex and the presence of PSCs possibly could lead to large differences between the two instruments. It was therefore decided to remove Antarctic and Arctic vortex measurements from the coincidence data set, by avoiding the periods December 2004–April 2005 (NH) and May 2005–September 2005 (SH). A total of 164 coincidences in the NH and 35 in the SH remained. On average, the distance between ACE and POAM III occultations is 400 km in the NH and 221 km in the SH.

The 525 nm ACE data cannot be directly compared with POAM III results since the latter has no channel at this wavelength. At 1020 nm, however, a direct comparison is possible with the 1018 nm POAM III channel. The statistical results for the coincidence data are shown in Fig. 8. Both data sets are in good agreement for the NH, but POAM III profiles are systematically higher below about 16 km in the SH. The comparison becomes more clear when we have a look at the relative differences in Fig. 9. Good agreement is indeed observed in the NH up to 21 km, above which ACE values are systematically higher than the POAM III ones. In the SH, ACE has lower values than POAM III below 16 km, while the situation reverses at higher altitudes.

4.5 OSIRIS comparisons

The Canadian OSIRIS instrument (Optical Spectrograph and InfraRed Imaging System), launched onboard the Odin satellite on 20 February 2001, measures the atmospheric limb radiance of scattered sunlight, using two subsystems (Llewellyn et al., 2004). First, an optical spectrograph (OS), consisting of a grating and a CCD detector, measures limb spectra in the 280–800 nm wavelength range with a 1 nm spectral resolution. Vertical profiles of the limb radiance are obtained by taking exposures while the instrument performs a repetitive vertical scan of the single line-of-sight through selected tangent altitude ranges from about 10 to 100 km, with successive measure-

ments taken at tangent altitudes with a spacing of roughly 2 km. About 60 scans per orbit can be obtained in this way, and global coverage of the Earth atmosphere is obtained in a few days. Second, an infrared imager (IRI), composed of three vertical linear array channels, captures one-dimensional images of the limb radiance at 1.26, 1.27 and 1.53 μm. In the context of this paper, only the measurements from the optical spectrograph are considered.

It is important to notice that limb scatter measurements differ fundamentally from transmittance measurements (GOMOS, POAM III, SAGE II, SAGE III). A transmittance value is determined by attenuation of the source light in the forward direction through absorption and scattering by the atmospheric species, and is therefore directly related to the optical extinction coefficient. A limb radiance value on the other hand is (in principle) determined by absorption and multiple scattering of light throughout all atmospheric layers in all directions, and it is therefore impossible to directly obtain the optical extinction coefficient in individual layers from limb measurements. For aerosols in particular, limb measurement retrievals focus directly on total particle number density and the particle size distribution. The latter is needed in the iterative retrieval process as it enters the radiative transfer forward model in the form of a scattering phase function (calculated with a Mie scattering code).

The OSIRIS aerosol retrieval process has been described in detail by Bourassa et al. (2007). First, all limb radiances are normalized with respect to the limb radiance at a reference altitude of 40 km to avoid the need for an absolute calibration and to provide some insensitivity to ground albedo. Then the ratio of the normalized radiance at 470 nm and 750 nm is calculated to render the measurements less sensitive to the assumed (and possibly wrong) neutral density. This ratio is inverted to particle number density with a Chahine-like inversion scheme, using the SASKTRAN radiative transfer model. A lognormal particle size distribution is assumed, with parameters taken from climatological SAGE II values. After inversion, the extinction coefficient is calculated from the solution. For the purpose of this paper, extinction coefficients at 525 nm and 1020 nm were evaluated from the retrieved number density and the assumed back-

ground log-normal size distribution.

Currently, OSIRIS aerosol products are not routinely processed. Therefore, coincident OSIRIS profiles had to be obtained separately from the limb radiance measurements. To avoid a large number of coincidences, a very small coincidence window was chosen: 2 h and 1 degree in circular distance on the Earth surface (about 110 km). The considered time period ranged from April 2004 (around the start of the ACE routine operations) to the point where the OSIRIS user data base was conveniently processed (August 2005). A total of 21 coincidences were found.

The statistics for ACE and OSIRIS profiles at both wavelengths are shown in Fig. 10. Once again, at 525 nm, ACE values are systematically negative above 25 km. They are also lower than the OSIRIS values at all altitudes, although both instruments are within reasonable agreement below 23 km. At 1020 nm, both instruments deliver very similar profile distributions, although ACE values are higher. The same conclusions can be drawn when we investigate the mean and standard deviation of the relative differences: a negative ACE bias at 525 nm below 23 km, and a positive ACE bias below 30 km.

5 Interpretation

After having compared the ACE imager extinction profiles with a variety of other instruments, a more o r less general picture emerges. Basically, 4 main observations can be made. (1) ACE aerosol extinction profiles are systematically negative for the visible channel at 525 nm, above about 23 to 25 km. The negative offset typically has a value of 5×10^{-5} to 1×10^{-4} km^{-1}. (2) The mean/median ensemble profiles and the relative difference profiles at 525 nm show good agreement in the upper troposphere/lower stratosphere below 20 to 25 km, with systematic differences that are sometimes positive, sometimes negative, but typically within 50 %. (3) At 1020 nm, relative difference profiles show good agreement between ACE and other instruments up to 20–25 km, but nearly always a positive bias is observed (with the notable exception for POAM III

below 16 km in the SH), with larger ACE values of a few percent in the troposphere and rising to 100% at 25 km. (4) For both wavelengths there is nearly always a NH/SH discrepancy present (with the exception of the SAGE III comparison) when looking at the median/mean profiles at both wavelengths in the troposphere/lower stratosphere region: NH comparisons are generally good, while SH mean extinction profiles for ACE are always smaller than the ones for the other instruments. Notice however that the difference between both instruments is not significant within the statistical spread of the profile ensembles. This is related to the remark given previously: the variability of aerosol extinction in the troposphere (and lower stratosphere, if we take PSCs into account) is very large.

It is far from easy to search for the physical/instrumental causes for the mentioned differences, especially since many factors are involved in calculation of the ACE aerosol extinction profiles. For the sake of clarity in the following reasoning, let us assume that the ACE-FTS gas retrievals and the gas cross sections are correct. Then, a negative offset aerosol extinction at 525 nm of (say) 7×10^{-5} km^{-1} implies that this offset occurs on the total extinction: $\beta_{\text{meas}} = \beta_{\text{true}} - a$ with $a=7\times10^{-5}$ km^{-1}. If $g(h, s)$ represents the path length of a light ray in an atmospheric segment ds, crossing at tangent altitude h, then the measured transmittance is:

$$T_{\text{meas}} = \exp\left(-\int g(h,s)(\beta_{\text{true}} - a)\mathrm{d}s\right) \quad (2)$$

$$= T_{\text{true}} \exp\left(a\int g(h,s)\mathrm{d}s\right) \quad (3)$$

The path length integral can be evaluated with a standard algorithm. For example, at a tangent altitude of 35 km, we get:

$$T_{\text{meas}} = T_{\text{true}} \exp(0.0625) = T_{\text{true}}(1 + 0.06) \quad (4)$$

Therefore, an extra light source term of about 6% is able to explain the observed negative offset. This value is in good agreement with values that Gilbert et al. (2007) report for the estimate of the multiple solar reflection contribution on the detectors: 5 to 8%.

On the other hand, it is far from clear why the relative difference profiles at 1020 nm show systematically higher values for ACE. The fact that the NIR images are out of focus should in principle leave the measured light intensity intact. The difference is therefore possibly induced by the linear increase in the detector response (or the non-perfect correction), an effect that was observed to be much more pronounced in the NIR imager (Gilbert et al., 2007). The smooth drift in altitude that is present in the relative difference profiles could be explained by this phenomenon.

The larger discrepancy for the median/mean extinction values at both wavelengths in the SH at lower altitudes are likely caused by PSCs and clouds in general. Particularly for the SAGE III and POAM III results, where PSC occurences were screened, a higher tropospheric cloud occurence may be responsible for the difference between ACE and the other measurements. A possible reason for the different ACE values can be found in the initial data processing. As already explained, solar images are rotated about their sun centroids before transmittance is calculated. However, when clouds are present, the solar disk is not well defined and has a very irregular shape (Dodion et al., 2007). It is possible, therefore, that the calculated rotation angle is not correct and erroneous transmittance profiles result.

6 Conclusions

The two imagers at 525 nm and 1020 nm onboard the ACE mission offer a promising and novel way to study aerosol and clouds in the Earth atmosphere, since it is in principle possible to derive 2-D aerosol extinction fields in a plane perpendicular to the line of sight. The novelty lies in the fact that particulate matter can be identified by the observed morphology (cloud shape, layers). At present, the algorithm for the imagers only use data from 3 pixels centered at the solar disk to derive total extinction profiles. We derived aerosol extinction profiles after subtraction of the gas contributions, provided by the ACE-FTS measurements. Comparisons with 3 independent solar occultation instruments (SAGE II, SAGE III, POAM III), one stellar occultation instrument

(GOMOS) and one limb sounder (OSIRIS) showed good agreement for the aerosol extinction in the upper troposphere/lower stratosphere region for both imagers. However, three problems remain to be handled. First, the aerosol extinction at 525 nm has a significant negative bias, probably due to extra light on the detector caused by multiple reflections of the solar image within the optics. Second, the NIR aerosol extinction profiles are systematically higher than the other measurements, possibly due to a (wrongly corrected) detector response that changes linearly during occultation. And third, the presence of clouds/PSCs in front of the solar disk could result in an erroneous aerosol extinction profile. Once these problems are tackled, the ACE imagers will offer very useful aerosol extinction profiles, ready to be exploited in scientific studies.

Acknowledgements. This study was funded by the PRODEX 7 contract SADE under the authority of the Belgian Space Science Office (BELSPO).

The Atmospheric Chemistry Experiment (ACE), also known as SCISAT, is a Canadian-led mission mainly supported by the Canadian Space Agency and the Natural Sciences and Engineering Research Council of Canada.

References

Bernath, P. F., McElroy, C. T., Abrams, M. C., Boone, C. D., Butler, M., Camy-Peyret, C., Carleer, M., Clerbaux, C., Coheur, P.-F., Colin, R., DeCola, P., DeMazière, M., Drummond, J. R., Dufour, D., Evans, W. F. J., Fast, H., Fussen, D., Gilbert, K., Jennings, D. E., Llewellyn, E. J., Lowe, R. P., Mahieu, E., McConell, J. C., McHugh, M., McLeod, S. D., Michaud, R., Midwinter, C., Nassar, R., Nichitiu, F., Nowlan, C., Rinsland, C. P., Rochon, Y. J., Rowlands, N., Semeniuk, K., Simon, P., Skelton, R., Sloan, J. J., Soucy, M. A., Strong, K., Tremblay, P., Turnbull, D., Walker, K. A., Walkty, I., Wardle, D. A., Wehrle, V., Zander, R., and Zou, J.: Atmospheric Chemistry Experiment (ACE): Mission overview, Geophys. Res. Lett., 32, L15S01, doi:10.1029/2005GL022386, 2005. 12350

Bertaux, J. L., Megie, G., Widemann, T., Chassefière, E., Pellinen, R., Kyrölä, E., Korpela, S., and Simon, P.: Monitoring of ozone trend by stellar occultations: The GOMOS instrument, Adv. Space Res., 11, 3237–3242, 1991. 12355

Bodhaine, B. A., Wood, N. B., Dutton, E. G., and Slusser, J. R.: On Rayleigh Optical Depth Calculations, J. Atmos. Oceanic Technol., 16, 1854–1861, 1999. 12354

Bogumil, K., Orphal, J., Voigt, S., Bovensmann, H., Fleischmann, O. C., Hartmann, M., Homann, T., Spietz, P., Vogel, A., and Burrows, J. P.: Reference Spectra of Atmospheric Trace Gases Measured by the SCIAMACHY PFM Satellite Spectrometer, in: Proc. 1st Europ. Sympos. Atmos. Meas. from Space (ESAMS-99), ISSN 1022-6656, 2, 443–447, ESA-ESTEC, Noordwijk, The Netherlands, 1999. 12354

Bourassa, A. E., Degenstein, D. A., Gattinger, R. L., and Llewellyn, E. J.: Stratospheric aerosol retrieval with OSIRIS Limb Scatter Measurements, J. Geophys. Res., 112, D10217, doi:10.1029/2006JD008079, 2007. 12362

Chu, W., McCormick, M., Lenoble, J., Brogniez, C., and Pruvost, P.: SAGE II inversion algorithm, J. Geophys. Res., 94, 8339–8351, 1989. 12357, 12358

Dodion, J., Fussen, D., Vanhellemont, F., Bingen, C., Mateshvili, N., Gilbert, K., Skelton, R., Turnbull, D., McLeod, S. D., Boone, C. D., Walker, K. A., and Bernath, P. F.: Cloud detection in the upper troposphere-lower stratosphere region via ACE imagers: A qualitative study, J. Geophys. Res., 112, D03208, doi:10.1029/2006JD007160, 2007. 12351, 12365

Fussen, D., Vanhellemont, F., Bingen, C., Kyrölä, E., Tamminen, J., Sofieva, V., Hassinen, S., Seppala, A., Verronen, P. T., Bertaux, J.-L., Hauchecorne, A., Dalaudier, F., Fanton d'Andon, O., Barrot, G., Mangin, A., Theodore, B., Guirlet, M., Renard, J.-B., Fraisse, R., Snoeij, P., Koopman, R., and Saavedra, L.: Autoregressive smoothing of GOMOS transmittances, Adv. Space Res., 36, 899–905, doi:10.1016/j.asr.2005.04.007, 2005. 12356

Gilbert, K. L., Turnbull, D. N., Walker, K. A., Boone, C. D., McCleod, S. D., Butler, M., Skelton, R., Bernath, P. F., Chateauneuf, F., and Soucy, M. A.: The On-Board Imagers for the Canadian ACE SCISAT-1 Mission, J. Geophys. Res., 112, D12207, doi:10.1029/2006JD007714, 2007. 12351, 12352, 12353, 12364, 12365

Kyrölä, E., Tamminen, J., Leppelmeier, G., Sofieva, V., Hassinen, S., Bertaux, J., Hauchecorne, A., Dalaudier, F., Cot, C., Korablev, O., Fanton d'Andon, O., Barrot, G., Mangin, A., Theodore, B., Guirlet, M., Etanchaud, F., Snoeij, P., Koopman, R., Saavedra, L., Fraisse, R., Fussen, D., and Vanhellemont, F.: GOMOS on Envisat – an overview, Adv. Space Res., 33, 1020–1028, 2004. 12355

Llewellyn, E. J., Lloyd, N. D., Degenstein, D. A., Gattinger, R. L., Petelina, S. V., Bourassa, A. E., Wiensz, J. T., Ivanov, E. V., McDade, I. C., Solheim, B. H., McConnell, J. C., Haley, C. S., von Savigny, C., Sioris, C. E., McLinden, C. A., Griffioen, E., Kaminski, J., Evans,

W. F. J., Puckrin, E., Strong, K., Wehrle, V., Hum, R. H., Kendall, D. J. W., Matsushita, J., Murtagh, D. P., Brohede, S., Stegman, J., Witt, G., Barnes, G., Payne, W. F., Piché, L., Smith, K., Warshaw, G., Deslauniers, D. L., Marchand, P., Richardson, E. H., King, R. A., Wevers, I., McCreath, W., Kyrölä, E., Oikarinen, L., Leppelmeier, G. W., Auvinen, H., Mégie, G., Hauchecorne, A., Lefèvre, F., de La Nöe, J., Ricaud, P., Frisk, U., Sjoberg, F., von Schéele, F., and Nordh, L.: The OSIRIS instrument on the Odin spacecraft, Canadian J. Phys., 82, 411–422, doi:10.1139/P04-005, 2004. 12361

Lucke, R. L., Korwan, D., Bevilacqua, R. M., Hornstein, J. S., Shettle, E. P., Chen, D. T., Daehler, M., Lumpe, J. D., Fromm, M. D., Debrestian, D., Neff, B., Squire, M., König-Langlo, G., and Davies, J.: The Polar Ozone and Aerosol Measurement (POAM III) Instrument and Early Validation Results, J. Geophys. Res., 104, 785–799, 1999. 12360

McElroy, C. and et al.: The ACE-MAESTRO instrument on SCISAT: description, performance, and preliminary results, Appl. Optics, 46, 4341–4356, 2007. 12350

Randall, C. E., Bevilacqua, R. M., Lumpe, J. D., and Hoppel, K. W.: Validation of POAM III aerosols: Comparison to SAGE II and HALOE, J. Geophys. Res., 106, 27 525–27 536, 2001. 12360

Rind, D., McCormick, M., and the SAGE III ATBD team: SAGE III Algorithm Theoretical Basis Document (ATBD) Solar and Lunar Algorithm, Tech. rep., 2002. 12359

Russell, P. B. and McCormick, M. P.: SAGE II Aerosol Data Validation and Initial Data Use: An Introduction and Overview, J. Geophys. Res., 94, 8335–8338, 1989. 12351

Thomason, L., Poole, L., and Randall, C.: SAGE III aerosol extinction validation in the Arctic winter: comparisons with SAGE II and POAM III, Atmos. Chem. Phys., 7, 1423–1433, 2007, http://www.atmos-chem-phys.net/7/1423/2007/. 12358

Yue, G. K., C. H. L. and Wang, P. H.: Comparing aerosol extinctions measured by Stratospheric Aerosol and Gas Measurement (SAGE) II and III satellite experiments in 2002 and 2003, J. Geophys. Res., 110, D11202, doi:10.1029/2004JD005421, 2005. 12358, 12359

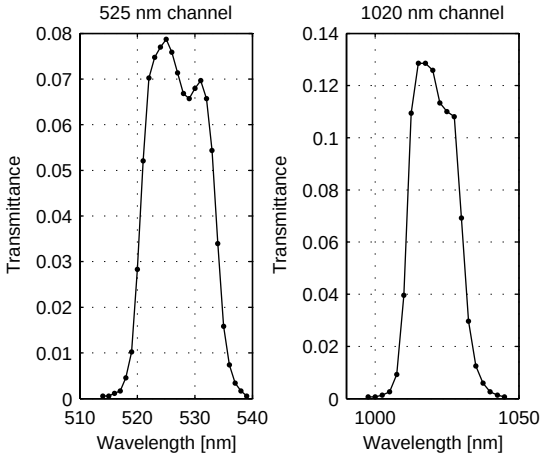

Fig. 1. Normalized filter functions of the 525 nm and 1020 nm imager channels.

ACPD
7, 12349–12379, 2007

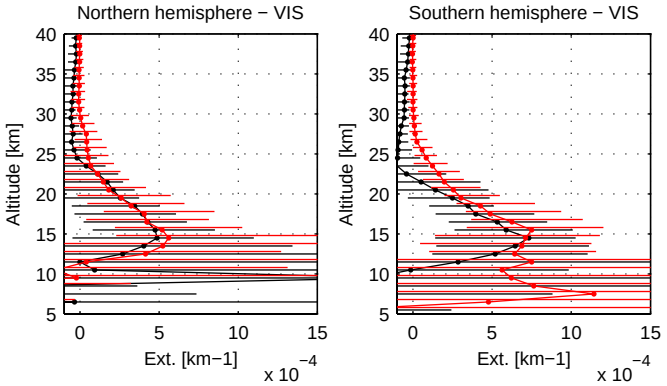

Fig. 2. Coincidence data set: median ACE (black) and GOMOS (red) 525 nm aerosol extinction profiles for the NH and SH. The spread of the data set around the median (16th and 84th percentile) is shown with horizontal lines.

ACPD
7, 12349–12379, 2007

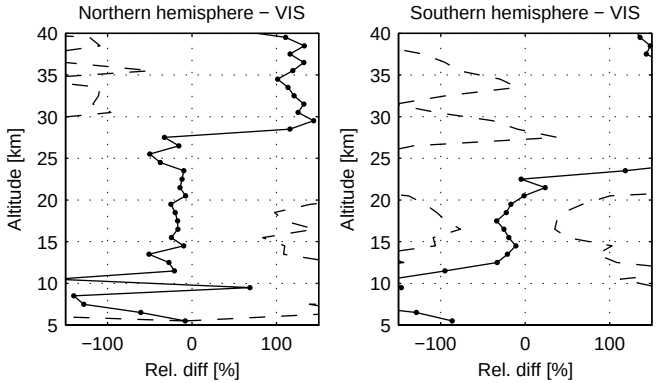

Fig. 3. Median (solid line), 16th and 84th percentile (dashed lines) of the relative difference between ACE and GOMOS for the NH and SH at 525 nm.

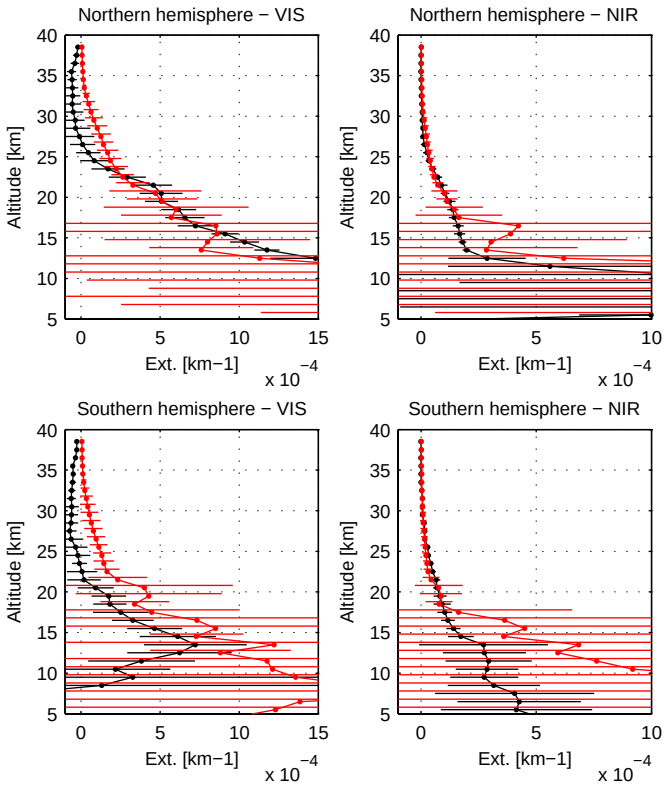

Fig. 4. Coincidence data set: mean ACE (black) and SAGE II (red) aerosol extinction profiles for the NH and SH. Left column: Visible channel. Right column: NIR channel. The spread of the data set around the mean is shown with horizontal lines (one standard deviation).

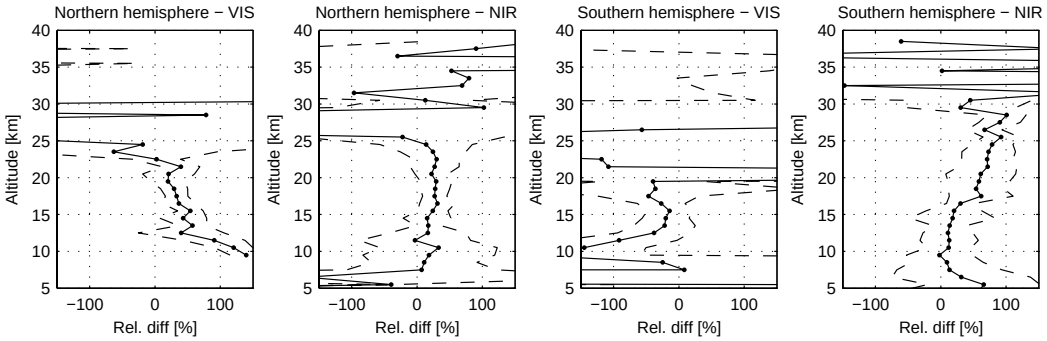

Fig. 5. Mean (solid line) and standard deviation (dashed lines) of the relative difference between ACE and SAGE II for the NH and SH at both imager wavelengths.

ACPD
7, 12349–12379, 2007

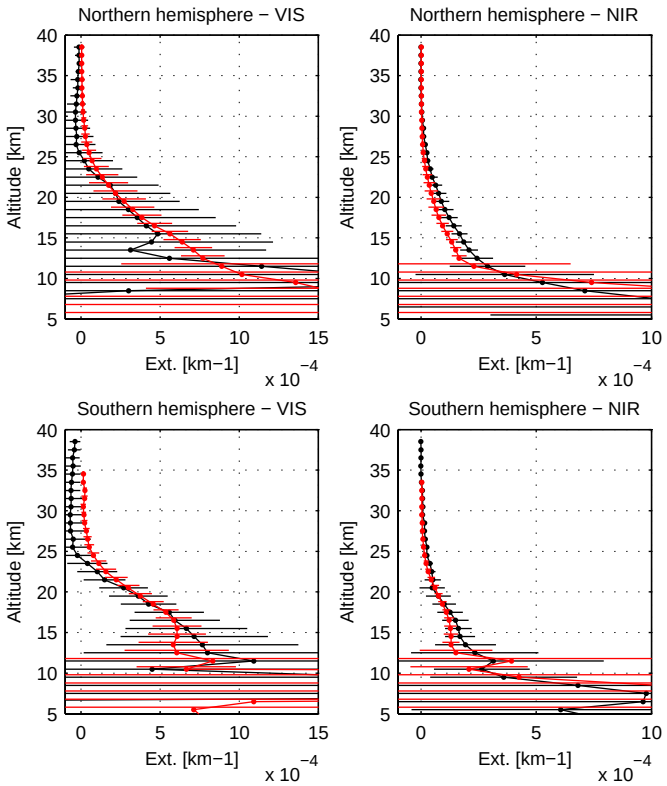

Fig. 6. Coincidence data set: mean ACE (black) and SAGE III (red) aerosol extinction profiles for the NH and SH. Left column: Visible channel (525 nm). Right column: NIR channel (1020 nm). The spread of the data set around the mean is shown with horizontal lines (one standard deviation).

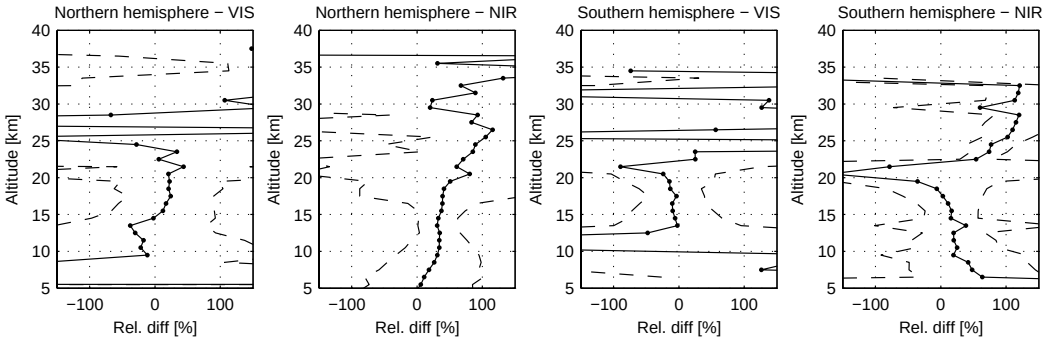

Fig. 7. Mean (solid line) and standard deviation (dashed lines) of the relative difference between ACE and SAGE III for the NH and SH at both imager wavelengths.

ACPD
7, 12349–12379, 2007

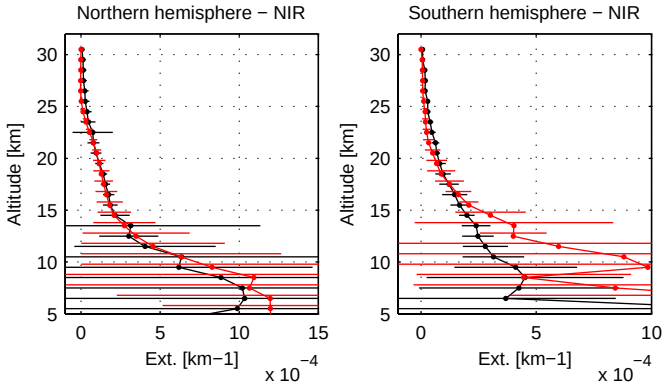

Fig. 8. Coincidence data set: mean ACE (black) and POAM III (red) aerosol extinction profiles at 1020 nm. Left: NH. Right: SH. The spread of the data set around the mean is shown with horizontal lines (one standard deviation).

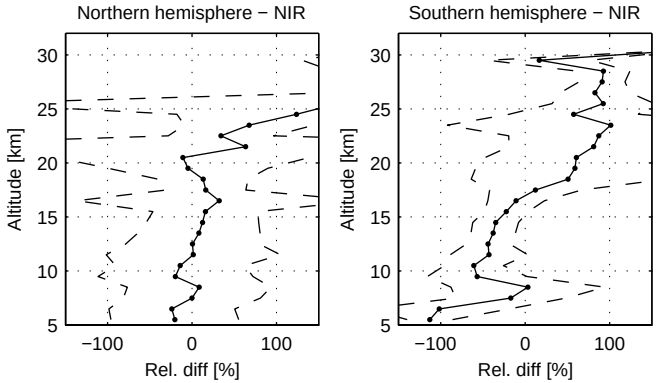

Fig. 9. Mean (solid line) and standard deviation (dashed lines) of the relative difference between ACE and POAM III for the NH and SH at 1020 nm.

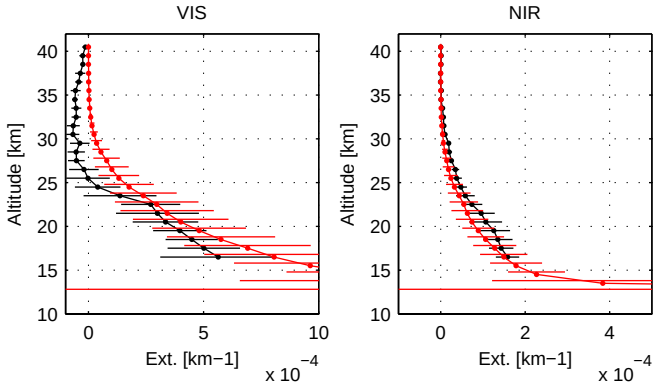

Fig. 10. Coincidence data set: mean ACE (black) and OSIRIS (red) aerosol extinction profiles. Left column: Visible channel (525 nm). Right column: NIR channel (1020 nm). The spread of the data set around the mean is shown with horizontal lines (one standard deviation).

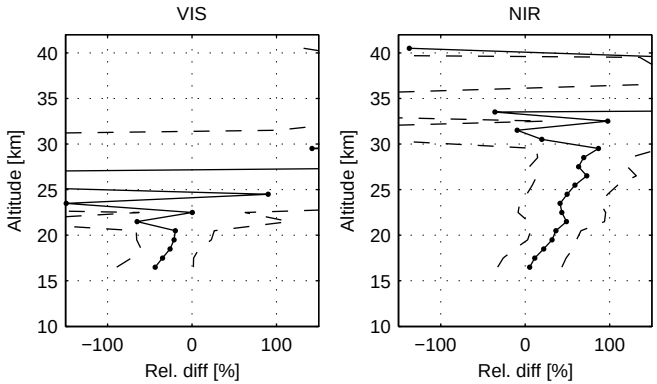

Fig. 11. Mean (solid line) and standard deviation (dashed lines) of the relative difference between ACE and OSIRIS for the NH and SH at both imager wavelengths.

ACPD
7, 12349–12379, 2007